CFD Letters

CFD Prediction of B-Series Propeller Performance in Open Water

Open Access

Ahmad Fitriadhy[1,*], Nur Amira Adam[2], C.J. Quah[3], Jaswar Koto[4], Faisal Mahmuddin[5]

[1] Faculty of Ocean Engineering Technology and Informatics, Universiti Malaysia Terengganu, 21030 Kuala Terengganu, Terengganu, Malaysia
[2] Postgraduate Student, Faculty of Ocean Engineering Technology and Informatics, Universiti Malaysia Terengganu, 21030 Kuala Terengganu, Terengganu, Malaysia
[3] CEO Numit Enterprise, Seri Kembangan, Selangor, Malaysia
[4] Department of Aeronautical, Automotive and Ocean Engineering, Universiti Teknologi Malaysia, Johor Bahru, Malaysia
[5] Marine Engineering Department, Engineering Faculty, Hasanuddin University, Makassar, Indonesia

ARTICLE INFO	ABSTRACT
	In presence of hydrodynamics interactions between propeller and velocity fields, it may lead to inaccurate prediction of the propeller's quantities such as thrust, torque, and its efficiency. This paper presents a Computational Fluid Dynamics (CFD) simulation approach to predict the thrust (K_T), torque (K_Q) and efficiency (η) coefficients in open-water condition. The scale model of propeller with various blade numbers (Z) have been appropriately taken into account within the range of advance number $0.1 \leq J \leq 1.05$. Here, B-series model propeller has been employed in computational simulation. In general, the results revealed that the subsequent increase of blade numbers has been proportional with the magnitude of K_T and K_Q of the propeller. However, it was inversely proportional to the propeller efficiency coefficient (η); where the highest efficiency value was 89% occurred at $Z=3$. This CFD simulation provides a preliminary prediction of the propeller characteristics.

1. Introduction

The marine propeller has the characteristics of a complex structure consisting of the hub and the blades. As the main component, the propeller blade is composed of irregular surfaces such as the suction and pressure side; which is greatly affects the propeller performance. Since almost 70% of the power from the engine was delivered to the propulsion system, the proper propeller design may contribute to increased propeller efficiency and directly reduced the power consumption [1]. Accordingly, a reliable approach of the propeller's prediction should be firmly proposed quantifying the accurate properties of thrust, torque and efficiency coefficients with respect to the ship's speed during sailing.

Several researchers have conducted both theoretical and experimental approaches to predict the propeller characteristics in open water. Referring to Epps, Ketcham [2], Ekinci [3] and Rahman, Ullah

---

* Corresponding author.
E-mail address: a.fitriadhy@umt.edu.my (Ahmad Fitriadhy)

[4], the theoretical prediction of propeller performance was conducted according to circulation or lifting line theory. However, this theoretical approach has some inaccurate prediction where a few parameters were omitted. Meanwhile, some researchers [5-7] have carried out experimental approach at towing tank at various configurations test model; in fact, it is relatively expensive, time-consuming, and have a complex procedure. To overcome such problem, a reliable solution through applying Computational Fluid Dynamics (CFD) simulation can be an alternative approach as well as have good agreement as compared to experimental results [8-12].

This paper presents a CFD simulation as the extension work from Fitriadhy and Adam [13] and Fitriadhy, Razali [14] to assess the propeller performance quantified by thrust (K_T) and torque (K_Q) and its efficiency (η) coefficients. In this computational simulation, several numbers of blades have been considered where the result of K_T, K_Q and η have been comprehensively discussed and presented through the magnitude of scalar torque and static pressure. The type of B-series model has been appropriately taken into account within the range of advance ratio 0.1≤J≤1.05. Here, CFD software of Fine[TM]/Turbo is utilized in the current simulation. The package of CFD including Autogrid5[TM] to generate fully hexahedral grid generation, 3D Reynolds Averaged Euler and Navier Stokes flow solver EURANUS and CFView[TM] as a post-processing module to visualize the results [15].

2. Theoretical Background

2.1 Governing Equation

The cornerstone of computational fluid dynamics application, there is consist of fundamental mathematical equations such as continuity, momentum and energy conservation equation. CFD flow solver (ISIS-CFD) on Numeca Fine[TM]/Turbo was based on the incompressible unsteady Reynolds-Averaged Navier-Stokes equation (URANSE) in which the solver applied the Finite Volume Method (FVM) for representing the inflow and outflow areas, where the fluid flow is well behaved.

2.2 Conservation Equation

To carry out the application of general conservation form of the Navier-Stokes equation using FVM, the model of a finite volume has been considered fixed in space and the fluid element is moving. The mass continuity equation in conservation form is based on steady and constant density of incompressible flows was presented in Eq. (1). Here, the ρ is the density, U_i is the averaged Cartesian components of the velocity-vector in i[th] direction (i=1,2,3) [16].

$$\frac{\partial}{\partial_{xi}}(\rho u_i) = 0 \tag{1}$$

Newton's 2nd law has been applied in FVM to a model of the fluid flow. When the fluid element moving, the net force on the fluid element equals its mass times the acceleration of the element. Therefore, the global Navier-Stokes equation applied the principle of the linear momentum conservation to solve the problem as expressed in Eq. (2).

$$\frac{\partial}{\partial_{xi}}(\rho u_i) + \frac{\partial}{\partial_{xj}}\left(\rho u_j \rho u_i\right) = -\frac{\partial p}{\partial x_i} + \frac{\partial \tau_{ij}}{\partial x_i} + \rho g_i + F_i \tag{2}$$

where p is the static pressure, g_i is the gravitational acceleration, F_i is an external body force in an averaged Cartesian component of the velocity-vector in i[th] direction (i=1,2,3) and δ_{ij} is the Kroneker delta and is equal to unity $i = j$ and zero when $i \neq j$.

2.3 Turbulence Model

During the simulation, a simple one-equation model has relatively applied to compute rotating motions of propeller. The Spalart-Allmaras transports equation model made for eddy viscosity and not required finer grid resolution to capture the velocity field gradients with algebraic models [17-20]. For external flow application, the kinematic turbulent $v_t (m^2/s)$ in this model can be specified and estimate based on the assumptions, $v_t/v = 1$ [15]. Here, the transport model for the working variable is shown in Eq. (3).

$$\frac{\partial \rho \tilde{v}}{\partial t} + \frac{\partial \rho u_j \tilde{v}}{\partial x_j} = \frac{\partial}{\partial x_j}\left[\left(\mu + \frac{\mu_\tau}{\sigma}\right)\frac{\partial \tilde{v}}{\partial x_j}\right] + c_{b2}\frac{\partial \tilde{v}}{\partial x_j}\frac{\partial \rho \tilde{v}}{\partial x_j} + c_{b1}\rho \widetilde{W}\tilde{v} - c_{w1}f_w\rho\left(\frac{\tilde{v}}{y}\right) \tag{3}$$

The eddy viscosity and damping function is defined as Eq. (4) and (5) respectively. Where, $X = \frac{\tilde{v}}{v}$ and the kinematic viscosity $v = \mu/\rho$.

$$\mu_\tau = f_{v1}\rho\tilde{v} \tag{4}$$

$$f_{v1} = \frac{X^3}{X^3 + c_{v1}{}^3} \tag{5}$$

It should be noted here that the best practice in turbulence model quantities by considering an appropriate grid to estimate the cell meshing size, y_{wall} as written in Eq. (6) below.

$$y_{wall} = 6\left(\frac{V_{ref}}{v}\right)^{-\frac{7}{8}}\left(\frac{L_{ref}}{2}\right)^{\frac{1}{8}}y_1 \tag{6}$$

Note that the reference velocity, V_{ref}, can be taken from the body velocity. The reference length, L_{ref}, should be based on the body length since an estimation of the boundary layer thickness is implied in this calculation.

2.4 Hydrodynamics Theory of Propeller

The propeller model has been tested in open water to determine the intrinsic propeller performance. The computed result from CFD usually refers to thrust (T), torque (Q) and efficiency (η). Thus, the performance data are given as form dimensionless thrust (K_T) and torque (K_Q) coefficients to plotted against the advance ratio (J). The dimensionless quantities are defined as Eq. (7)-(10).

$$J = \frac{v_a}{n.D} \tag{7}$$

$$K_T = \frac{T}{\rho n^2 D^4} \tag{8}$$

$$K_Q = \frac{Q}{\rho n^2 D^5} \tag{9}$$

$$\eta = \frac{J}{2\pi}\frac{K_T}{K_Q} \tag{10}$$

where ρ is the water density, n the number of propeller rotations per second (RPS), D the propeller diameter and v_a represents for water advance velocity (m/s).

3. Simulation Condition
3.1 Principal Data of Propeller

The principal dimensions of the scale model propeller are presented in Table 1.

Table 1
Principle dimensions of propeller

Geometrical parameters	Full Scale	Model Scale
Diameter (mm)	3650	119.25
AE/AO	0.695	0.695
P/D	1.013	1.013
Pitch (mm)	3697.45	120.83
Scale	1:30.6	
Propeller Orientation	Right-hand rotation	

3.2 Parametric Studies

As mentioned earlier, several blade numbers (Z) associated with various advance ratios from 0.10 up to 1.05 have been taken into consideration. The details of simulation parameters are completely summarized in Table 2.
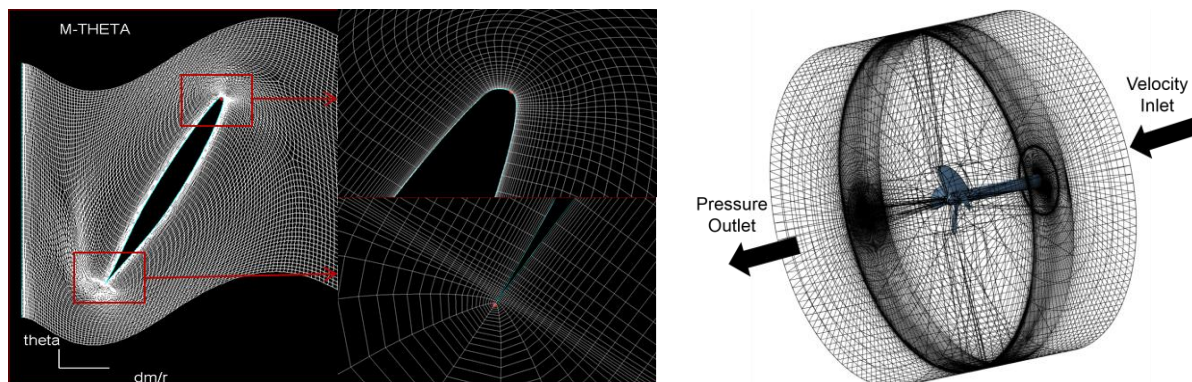
Table 2
The simulation conditions

Propeller revolution (RPM)	Blade Number (Z)		
	Z=3	Z=4	Z=5
1200	√	√	√

4. Computational Domain and Mesh Generation

The CFD simulation of propeller performance in open-water condition has been developed at Numeca Fine™/Turbo software. The geometry of propeller required to define the blade and hub structure to generate an automatic mesh. This simulation only considered a single blade of the propeller and another blades are performed by using a rotational periodicity (blade numbers) to save the computational time [21].

During this meshing process, the rounded streamwise O4H grid topology type with 97 grid points in the pitchwise direction has been selected according to the geometry configuration and grid level [15]. The grid generated in meshing phase are using 2.8 million nodes number for this scale model and the first cell size is set with 1.0µm for the blades and hub surface. Therefore, the grid generated able to maintain the non-dimensional wall distance y^+ as below 1.5 for all solid surface. To increase the computation accuracy, a local mesh refinement is required by decreases the grid size when the cell near the blades walls to capture a large pressure gradient occurs near to the wall as displayed in Figure 1 (left) [22]. The velocity inlet was specified as having a constant velocity of the flow model and a static pressure has been imposed at outlet boundary as shown in Figure 1 (right). The value for rotational speed of the solid boundary condition types (blades and hub) was set as negative value to indicates a propeller rotational in negative θ-direction according to a right handed propeller orientation [15]. Since this computational have complex fluid problem, the Merkle preconditioner

has been selected to increase the convergence rate and computation efficiency at very low flow speed [21, 23].

Fig. 1. Local refinement of the block structured (left) and inlet and outlet location in domain (right) for Z=4 mesh model

Four different of the propellers meshes are summarized in Table 3, was created in AutoGrid5^{TM}. This mesh independency has been generated in order to ensure an adequate number of cells meshing that were sufficiently used for all simulation to obtain an accuracy and steadiness in the computational result regardless of the longer CPU time. Here, the total number of cells meshing with 2,817,090 was selected for all simulation due reliability mesh result to capturing the flow filed and pressure distribution on blade's surface. The increase of the total number of cells meshing up to 4,000,666 was unnecessary due to insufficient impact with longer computation time. In the final stage of the CFD simulation, a graphical result will be generated using CFView^{TM} to visualize the scalar torque and static pressure for all various configurations of the propeller as displayed in Figure 2. Having considered the proper total number of the meshes, the initial CFD simulation has been successfully performed. Here, the result has well agreements with experimental model test as completely presented in Table 4, where the percentage discrepancy error of K_T, K_Q and η between the experimental and CFD results in acceptable range were about 1.04%, 2.24% and 1.23%, respectively.

Table 3
Mesh Independent study on propeller geometry

Case	J	Total number of cell meshing	$10K_Q$	K_T	η
A	0.5	1,789,042	0.44371	0.27545	0.49402
B		2,559,546	0.44223	0.27628	0.49715
C		2,817,090	0.43853	0.27450	0.49821
D		4,000,666	0.43875	0.27616	0.50089

Table 4
CFD and experimental results associated with Z=4 and RPM=1200

J	$10K_Q$			K_T			η		
	CFD	EXP	(%)	CFD	EXP	(%)	CFD	EXP	(%)
0.50	0.4385	0.4485	-2.238	0.2745	0.2774	-1.040	0.4982	0.4920	1.226

*Negative sign (-) means that the CFD result is lower than the experimental result
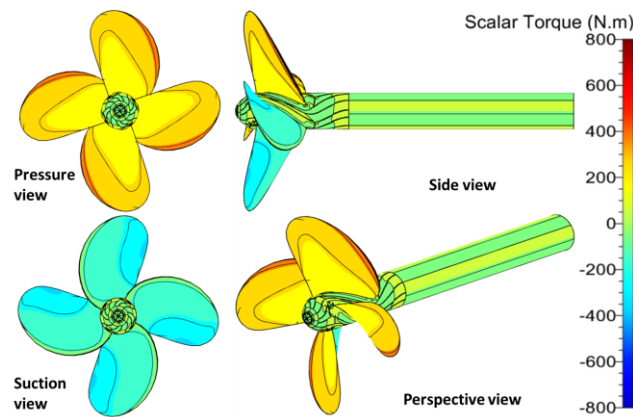
**Fig. 2.** Magnitude of scalar torque for pressure (left) and suction (right) side at J=0.5 and 1200 RPM

5. Results and Discussion

The analysis for thrust (K_T), torque (K_Q) and efficiency (η) coefficients of the propeller in the various blade numbers have been presented and appropriately discussed. In this study, the Computational Fluid Dynamics was adopted to obtain the propeller performance.

5.1 Effect of Various Blade Numbers (Z)

Referring to the CFD results, the torque and thrust coefficients relatively decreases as increases the advance ratio from 0.10 to 1.05 (see Figure 3). This can be explained through the change of the water velocity between the solid surface and fluid flow. The lowest axial velocity surrounding the propeller blade will be accelerated from low velocity a generate the significant changes of the water velocity [24]. The deduction of drag force on the blade surface has been formed at the higher advance ratio. Here, the propeller characteristics quantified by the dark yellow colour (high scalar torque) contour region on the pressure surface as presented in Figure 4 (left), (middle) and (right).

Furthermore, the propeller efficiency increases steadily at lower advance ratio (J=0.10) up to propeller optimum value (J=0.95) and it will be prone to decrease at higher at advance ratio (J=1.00 and 1.05) as shown in Table 5. This is occurred due to the reduction of blue colour contour region (low-pressure drag) at the pressure side of the blade surface. This is similar to what was reported by Colley [25] and Yeo, Sabatly [26], the blue colour region has been expanded at the suction side which led to decrease the propeller efficiency as displayed in Figure 5 (left), (middle) and (right).
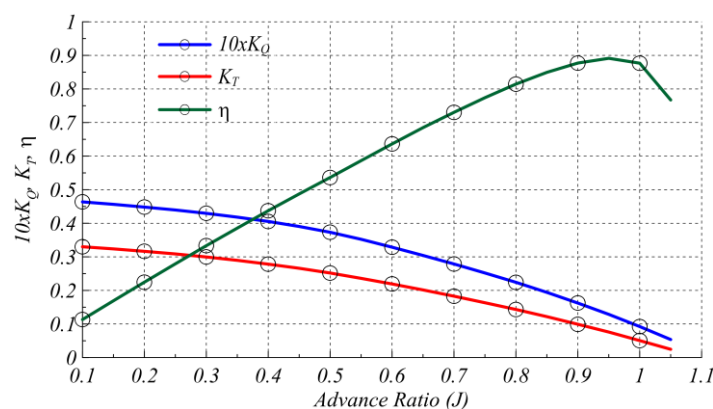
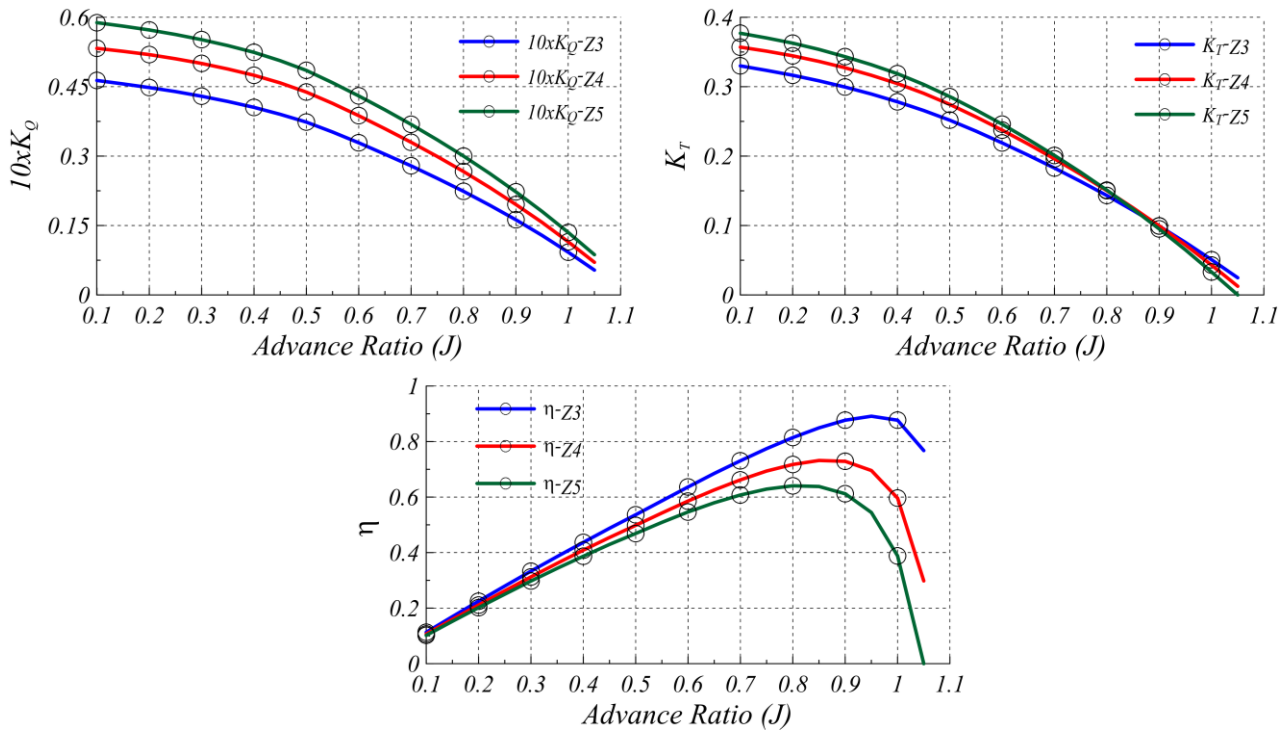**Fig. 3.** Thrust, torque and efficiency coefficients for Z=3 at the various advance ratio (J), RPM=1200
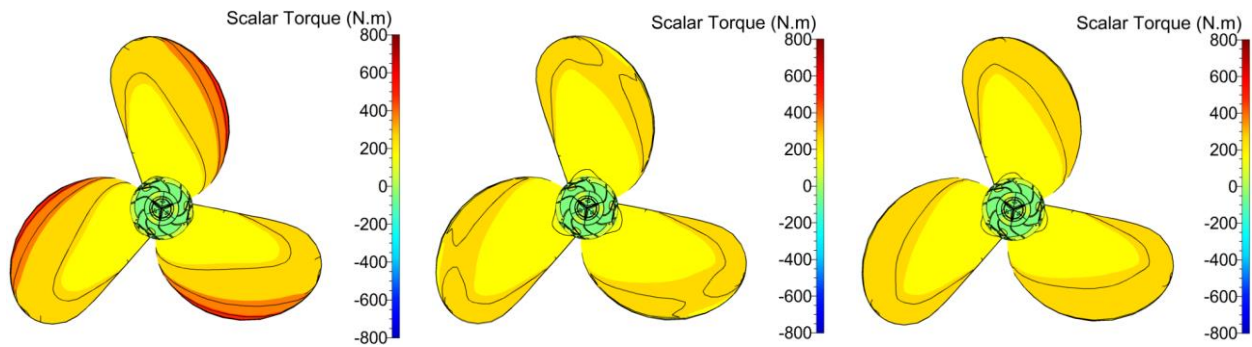
**Fig. 4.** Scalar torque at various advance ratio for 1200 RPM for J= 0.10 (left), J=0.95 (middle) and J=1.05 (right)
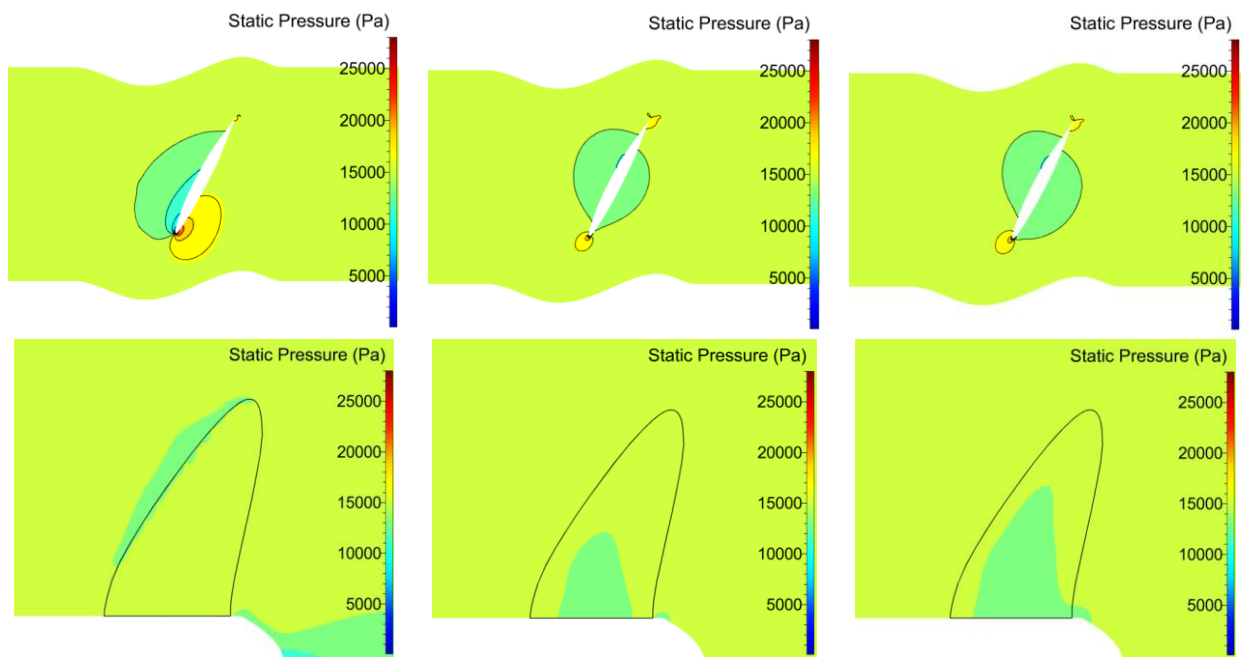
Fig. 5. Blade-to-Blade view (top) and meridional view (bottom) of static pressure at 1200 RPM for J= 0.10 (left), J=0.85 (middle) and J=1.05 (right)

In order to discuss the propeller performance for various blade numbers from 3 to 4 and 4 to 5, the simulation results show a significant influence on the torque, thrust and efficiency coefficients. Referring to Figure 6, the subsequent increases of blade number was proportional to the torque and thrust coefficients. This is also can be defined by the maximum percentage increments of $10K_Q$ and K_T; where the $10K_Q$ was 23.9 % (J=1.05) and 18.39% (J=1.05); while K_T was 92.3% (J=1.05) and 30.3% (J=1.0). The possible reason is due to the increase of the blade numbers will create more total blades area and produce high drag force, which is represented by dark-yellow (high scalar torque) colour regions as shown in Figure 7 (left), (middle) and (right) [24].

Fig. 6. Thrust coefficient, torque coefficient and efficiency for propeller at various number of blades (Z), RPM=1200
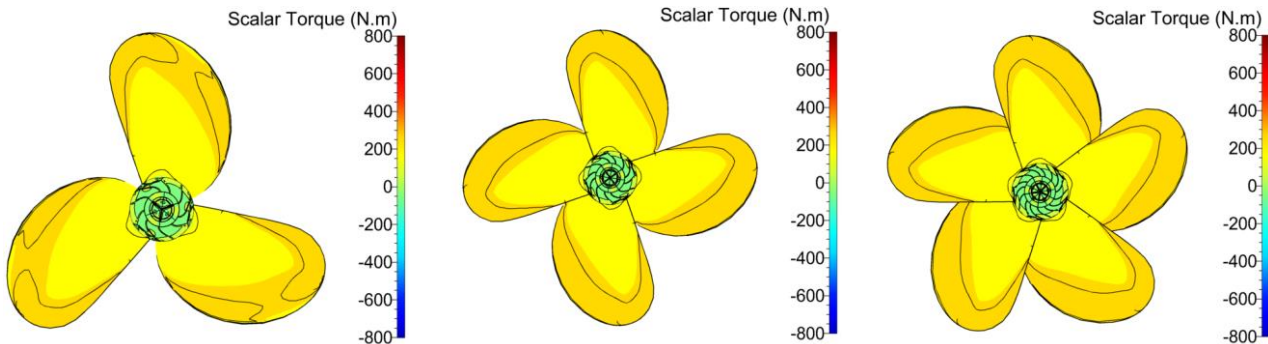

Fig. 7. Scalar torque of Z=3 (left), Z=4 (middle) and Z=5 (right) at J=0.95

However, the subsequent increase of blade number has produced a reduction of propeller efficiency with maximum percentage decrements 157.4% (J=1.05) and 53.6% (J=1.0), respectively. Since the additional surface area and drag force has been formed at higher blade number, it generates more low-pressure region around blade represented by green colour contour as displayed in Figure 8 (left), (middle) and (right) [27].

Consequently, it should be noted here the propeller with three blade number has provided the highest propeller efficiency by 89.1% at J=0.95 as compared to four (η =73.2% at J=0.85) and five (η =64.1% at J=0.80) blade numbers. In summary, it can be concluded that the torque and thrust coefficients were directly proportional to the blade numbers; while, the propeller efficiency was inversely proportional to the blade numbers. The maximum efficiency of the propeller generally occurred within the range of 0.8≤J≤0.95 regardless of the various blade numbers.
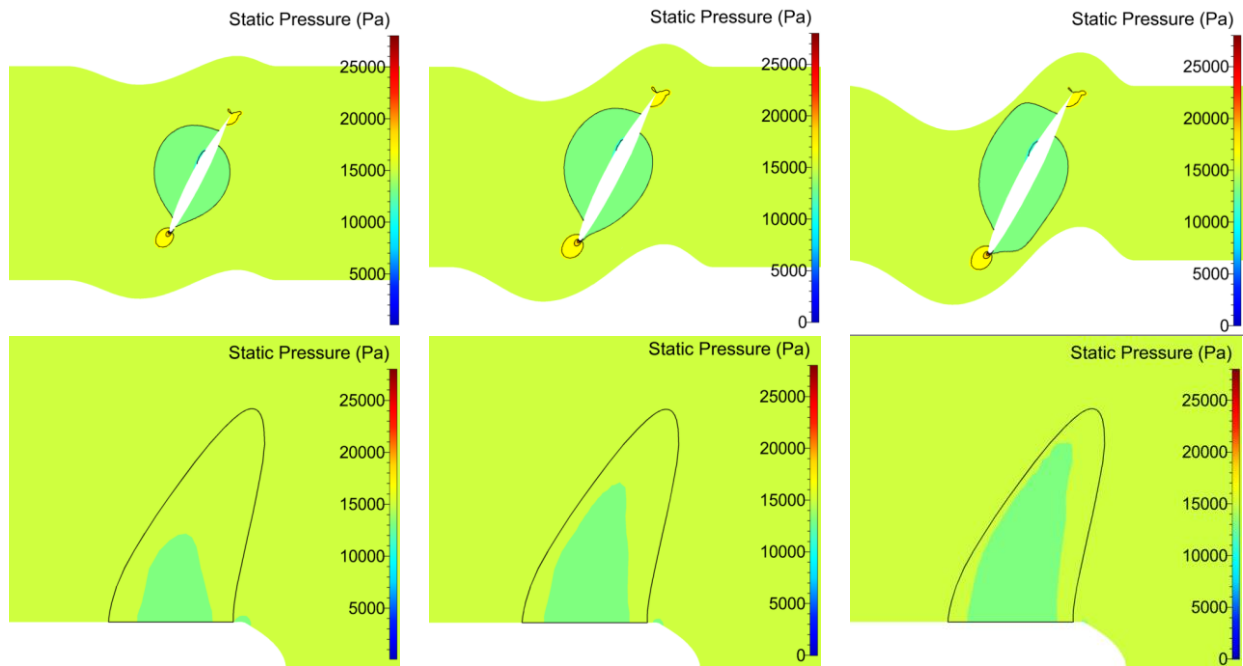
Fig. 8. Blade-to-Blade view (top) and meridional view (bottom) of static pressure at J=0.95 for Z=3 (left), Z=4 (middle) and Z=5 (right)

Table 5
Magnitude of thrust, torque and efficiency coefficients of propeller for Z=3, Z=4 and Z=5

J	Z = 3			Z = 4			Z = 5		
	$10K_Q$	K_T	η	$10K_Q$	K_T	η	$10K_Q$	K_T	η
0.10	0.463	0.330	0.113	0.533	0.357	0.107	0.588	0.377	0.102
0.15	0.456	0.323	0.169	0.526	0.351	0.159	0.581	0.370	0.152
0.20	0.448	0.316	0.225	0.519	0.345	0.211	0.573	0.363	0.202
0.25	0.439	0.309	0.279	0.511	0.337	0.262	0.563	0.354	0.250
0.30	0.429	0.300	0.333	0.500	0.327	0.312	0.552	0.343	0.297
0.35	0.418	0.289	0.386	0.488	0.317	0.361	0.539	0.332	0.343
0.40	0.405	0.278	0.437	0.475	0.305	0.408	0.524	0.319	0.387
0.45	0.390	0.266	0.487	0.458	0.291	0.454	0.506	0.303	0.429
0.50	0.373	0.252	0.536	0.438	0.275	0.498	0.485	0.286	0.469
0.55	0.352	0.236	0.586	0.414	0.257	0.543	0.459	0.266	0.509
0.60	0.329	0.219	0.637	0.387	0.238	0.586	0.430	0.246	0.546
0.65	0.304	0.201	0.685	0.359	0.217	0.626	0.400	0.224	0.579
0.70	0.279	0.183	0.730	0.330	0.196	0.662	0.369	0.201	0.607
0.75	0.252	0.163	0.774	0.299	0.174	0.693	0.335	0.177	0.629
0.80	0.224	0.143	0.814	0.267	0.150	0.717	0.300	0.151	0.641
0.85	0.194	0.122	0.849	0.232	0.125	0.732	0.262	0.124	0.638
0.90	0.162	0.099	0.877	0.195	0.099	0.729	0.223	0.095	0.612
0.95	0.129	0.076	0.891	0.157	0.072	0.696	0.180	0.065	0.545
1.00	0.092	0.051	0.877	0.115	0.043	0.596	0.135	0.033	0.388
1.05	0.054	0.025	0.767	0.071	0.013	0.298	0.087	0.000	0.000

6. Conclusion

The CFD simulation was successfully carried out using B-series model in open water condition where the effect of various blade numbers within the range of advance number 0.10 ≤J≤1.05 have been considered. The results have been drawn as follow

- The higher value of J leads to decrease the value of K_T and K_Q coefficients. Meanwhile, the value of propeller efficiency is prone to reduce at higher value of its advance number .
- The increase of blade number was proportional with the value of thrust and torque coefficients, but it reduces the efficiency as increase the blade numbers.
- The highest efficiency of the propeller incorporated with Z=3 is 89% with advance ratio J=0.95.

Acknowledgement

References

[1]   Bertram, Volker. *Practical ship hydrodynamics*. Elsevier, 2011.
[2]   Epps, Brenden, Jerod Ketcham, and Chryssostomos Chryssostomidis. "Propeller blade stress estimates using lifting line theory." In *Proceedings of the 2010 Conference on Grand Challenges in Modeling & Simulation*, pp. 442-447. Society for Modeling & Simulation International, 2010.
[3]   Ekinci, Serkan. "A practical approach for design of marine propellers with systematic propeller series." *Brodogradnja: Teorija i praksa brodogradnje i pomorske tehnike* 62, no. 2 (2011): 123-129.
[4]   Rahman, Ataur, Md Refayet Ullah, and Md Mashud Karim. "Marine Propeller Design Method based on Lifting Line Theory and Lifting Surface Correction Factors." *Procedia engineering* 194 (2017): 174-181.
[5]   Arazgaldi, R., A. Hajilouei, and B. Farhanieh. "Experimental and numerical investigation of marine propeller cavitation." *Sharif University of Technology, Journal SCIENTIA IRANICA* 16, no. 6 (2009): 525-533.
[6]   Taheri, Ramin, and Karim Mazaheri. "Hydrodynamic Optimization of Marine Propeller Using Gradient and Non-Gradient-based Algorithms." *Acta Polytechnica Hungarica* 10, no. 3 (2013): 221-237.
[7]   Elghorab, M. A., A. Abou El-Azm Aly, A. S. Elwetedy, and M. A. Kotb. "Experimental study of open water non-series marine propeller performance." In *Proceedings of world academy of science, engineering and technology*, no. 78, p. 924. World Academy of Science, Engineering and Technology (WASET), 2013.
[8]   Turunen, Tuomas, Timo Siikonen, Johan Lundberg, and Rickard Bensow. "Open-water computations of a marine propeller using OpenFOAM." In *ECFD VI-6th European Congress on Computational Fluid Dynamics, Barcelona, Spain, 20-25 July 2014*, pp. 1123-1134. 2014.
[9]   Felicjancik, Judyta, Sebastian Kowalczyk, Karol Felicjancik, and Krzysztof Kawecki. "Numerical simulations of hydrodynamic open-water characteristics of a ship propeller." *Polish Maritime Research* 23, no. 4 (2016): 16-22.
[10]   Nasution, Sanjaya Baroar Sakti, Budiarso Warjito, and Dendy Adanta. "A Comparison of Openflume Turbine Designs with Specific Speeds (Ns) Based on Power and Discharge Functions." *Journal of Advanced Research in Fluid Mechanics and Thermal Sciences* 51, no, 1 (2018): 53-60.
[11]   Fitriadhy, Ahmad, Nur Adlina Aldin, and Nurul Aqilah Mansor. "CFD Analysis on Course Stability of a Towed Ship Incorporated with Symmetrical Bridle Towline." *CFD Letters* 11, no. 12 (2019) 88-98.
[12]   Fitriadhy, Ahmad, Nurul Aqilah Mansor, Nur Adlina Aldin, and Adi Maimun. "CFD Analysis on Course Stability of An Asymmetrical Bridle Towline Model of a Towed Ship." *CFD Letters* 11, no. 12 (2019) 43-52
[13]   Fitriadhy, A., and N. Amira Adam. "Heave and pitch motions performance of a monotricat ship in head-seas." *International Journal of Automotive and Mechanical Engineering* 14 (2017): 4243-4258.
[14]   Fitriadhy, A., N. Razali, and N. AqilahMansor. "Seakeeping performance of a rounded hull catamaran in waves using CFD approach." *Journal of Mechanical Engineering and Sciences* 11, no. 2 (2017): 2601-2614.
[15]   Numeca, 2007, FINE/Turbo v8 User Manual, Numeca International, Brussels, Belgium.
[16]   Prakash, Senthil, and Deepthi R. Nath. "A computational method for determination of open water performance of a marine propeller." *International Journal of Computer Applications* 58, no. 12 (2012).
[17]   Deck, Sébastien, Philippe Duveau, Paulo d'Espiney, and Philippe Guillen. "Development and application of Spalart–Allmaras one equation turbulence model to three-dimensional supersonic complex configurations." *Aerospace science and technology* 6, no. 3 (2002): 171-183.
[18]   Kostić, Čedomir. "Review of the Spalart-Allmaras turbulence model and its modifications to three-dimensional supersonic configurations." *Scientific Technical Review* 65, no. 1 (2015): 43-49.
[19]   Hejlesen, Mads Mølholm, Johannes Tophøj Rasmussen, Allan Larsen, and Jens Honore Walther. "Implementation of the Spalart-Allmaras turbulence model in the two-dimensional vortex-in-cell method." In *6th European Congress on Computational Methods in Applied Sciences and Engineering*. Vienna University of Technology, 2012.

[20]   Lorin, Emmanuel, Amine Ben Haj Ali, and Azzeddine Soulaimani. "An accurate positivity preserving scheme for the Spalart-Allmaras turbulence model. Application to aerodynamics." In *36th AIAA Fluid Dynamics conference and exhibit*, p. 3743. 2006.

[21]   Martinez Javier, Piotr Doerffer, Oskar Szulc, and Fernando Tejero. "Aerodynamic analysis of wind turbine rotor blades." *Task Q* 19, no. 2 (2015): 129-140.

[22]   Kamal, Iwan Mustaffa, and Tuan Muhammad Amier Tuan Mohd Yusof. "A CFD RANS cavitation prediction for propellers." *ARPN Journal of Engineering and Applied Sciences* 12, no. 4 (2017): 1248-1253.

[23]   Folkner, David. "Improvement in computational fluid dynamics through boundary verification and preconditioning." *Utah State University* (2013).

[24]   Husaini, Muhamad, Zahurin Samad, and Mohd Rizal Arshad. "Autonomous underwater vehicle propeller simulation using computational fluid dynamic." *Computational Fluid Dynamics Technologies and Applications, InTech* (2011): 293-314.

[25]   Colley, Eamonn. "Analysis of Flow Around a Ship Propeller using OpenFOAM." *Curtin University, October* (2012).

[26]   Yeo, Kiam Beng, Rosalam Sabatly, Wen Yee Hau, and Cheah Meng Ong. "Effects of Marine Propeller Performance and Parameters Using CFD Method." *Journal of Applied Sciences* 14, no. 22 (2014): 3083-3088.

[27]   Boucetta, Djahida, and Omar Imine. "Numerical simulation of the flow around marine propeller series." *Journal of Physical Science and Application* 6, no. 3 (2016): 55-61.